

# Particle Transport Simulations of the Neutronic Performance of Moderators of the ESS Mercury Target-Moderator-Reflector System

D. Filges<sup>1\*</sup>, R.-D. Neef<sup>1</sup>, K. Nünighoff<sup>1</sup>, C. Pohl<sup>1</sup>, B. Haft<sup>2</sup>, S. Bennington<sup>3</sup>

<sup>1</sup>*Institut für Kernphysik, Forschungszentrum Jülich GmbH, D-52425 Jülich, Germany*

<sup>2</sup>*Abt. Strahlenphysik, Institut für theoretische Physik, Technische Universität Graz, Steyrergasse 17, A-8010 Graz, Austria*

<sup>3</sup>*ISIS facility, Rutherford Appleton Laboratory, Chilton, Didcot, Oxon, OX11 0QX, United Kingdom*

## INTRODUCTION

In this report we describe the ongoing work on the Monte Carlo simulations (see also [1,2]) of the neutron performance for the ESS target stations. Detailed simulations of the wavelength dependent time distributions of the neutrons leaving the moderator surface are performed. The emphasis of the simulations is in accordance to the outcome of a meeting of neutron scattering scientists at Heathrow in February 2001 [4]. We present our results for the below listed moderator setups:

### 1. short pulse (1 $\mu$ s)

- coupled cold (20 K) liquid hydrogen moderator
- decoupled cold hydrogen moderator
- decoupled-poisoned cold hydrogen moderator
- coupled ambient temperature water moderator
- decoupled ambient temperature water moderator
- decoupled-poisoned temperature water moderator
- coupled solid methane moderator
- decoupled solid methane moderator

### 2. long pulse (1 $\mu$ s)

- coupled cold hydrogen moderator

Furthermore we compare our recent results to the estimated neutronic performance of the SNS [5,6]. The performance of miscellaneous moderators like a grooved moderator or a solid methane moderator is also discussed. In each simulation we consider the bottom upstream moderator position as described in the ESS reference design [3]. The midpoint position of the considered moderators is 10 cm downstream from the mercury window interface. At the three other moderator positions H<sub>2</sub>O-moderators are placed. In the simulations we use a pure lead reflector, which is comparable to the real reflector with 15 Vol-% D<sub>2</sub>O cooling. The reflector has a height of 180 cm and a radius of 90 cm. The used set of parameters is listed in Tab. 1.

Table 1: Beam parameters used in the Monte-Carlo simulations.

|                    |  |                       |                       |
|--------------------|--|-----------------------|-----------------------|
| beam energy        | 1.334 GeV  |                       |                       |
| beamprofile        | elliptic beam, gaussian distributed<br>$r_x = 11 \text{ cm}, s_x = 3.67 \text{ cm}$<br>$r_y = 5 \text{ cm}, s_y = 1.67 \text{ cm}$ |                       |                       |
| average current    | $3.75 \text{ mA} = 2.34 \cdot 10^{16} \text{ p/s}$   |                       |                       |
| pulse frequency    | 10 Hz  | 16.7 Hz               | 50 Hz                 |
| average beam power | 1 MW   | 5 MW                  | 5 MW                  |
| proton per pulse   | $4.684 \cdot 10^{14}$  | $1.405 \cdot 10^{15}$ | $4.684 \cdot 10^{14}$ |
| pulse width        | 1 $\mu\text{s}$  | 2ms                   | 1 $\mu\text{s}$       |

The presented data are normalized per sr, per s, per Å, per pulse, and per cm<sup>2</sup>. A detailed description can be found in [2]. The output data from the simulation program are normalized as listed below:

- short pulse (50 Hz)

- peak current density:  $\frac{4.684 \cdot 10^{14} \text{ protons}}{10^{-6} \text{ s} \cdot 180 \text{ cm}^2 \cdot 2\mathbf{p} \cdot \Delta\mathbf{l}}$

- integral current density:  $\frac{4.684 \cdot 10^{14} \text{ protons} \cdot 50 \text{ s}^{-1}}{180 \text{ cm}^2 \cdot 2\mathbf{p} \cdot \Delta\mathbf{l}}$

- long pulse (16.7 Hz)
- peak current density:  $\frac{1.405 \cdot 10^{15} \text{ protons}}{10^{-6} \text{ s} \cdot 180 \text{ cm}^2 \cdot 2\mathbf{p} \cdot \Delta I}$
- integral current density:  $\frac{1.405 \cdot 10^{15} \text{ protons} \cdot 16.7 \text{ s}^{-1}}{180 \text{ cm}^2 \cdot 2\mathbf{p} \cdot \Delta I}$

In the simulations the neutron current leaving the viewed moderator surface is tallied. We determine the current in a solid angle of  $\pm 2^\circ$ , which is equivalent to the solid angle at a point in a distance of 2 m from the viewed moderator surface. It was not possible to obtain the wavelength dependent time spectra for neutrons leaving the surface within an angle of  $\pm 2^\circ$  to the surface normal, because of low statistics. But the statistics of the time spectra of thermal neutrons ( $E_{\text{kin}} < 0.383 \text{ eV}$ ) leaving the moderator is sufficient to determine the ratio between the integrated neutron current for a solid angle of  $2\pi$  and  $4^\circ$ . This factor was determined for each moderator configuration. The time spectra for a solid angle of  $2\pi$  are scaled with these factors.

## **COLD HYDROGEN MODERATOR**

In contrast to the geometry used in [2] in these simulations an extended premoderator was used, as shown in Fig. 1. The thickness of the water premoderator is 2 cm, and the thickness of the hydrogen moderator is 5 cm. The length of the extension is about 12 cm and has an optimized length in accordance to the results of [7].

In all simulations pure para-hydrogen was used. Fig. 2 shows the time distribution of the neutron current density for wavelengths of 2, 4, 6, and 10 Å for a cold coupled hydrogen moderator, and Fig. 3 for a decoupled hydrogen moderator. The numerical values for both moderators for the considered wavelengths are given in Tab. 2 and 3. The moderator was decoupled with an 1 mm Cd-layer on the inner surface of the neutron flight path. It can be seen that decoupling causes a slight decrease in intensity and peak-widths. Smaller peak-widths can be achieved by poisoning the decoupled hydrogen moderator. The time distributions of the neutron current density of a decoupled-poisoned hydrogen moderator is shown in Fig. 4. The poisoning is done with a 0.5 mm thick Gd-layer in the midplane of the hydrogen moderator vessel. The integrated neutron current

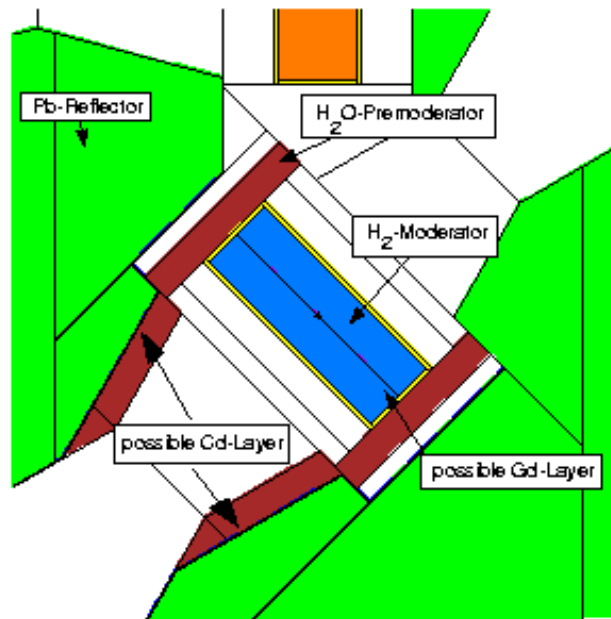


Fig. 1: Geometry of the H<sub>2</sub>-moderator with extended premoderator as used in the simulations. The moderator can be decoupled with a Cd-layer on the inner side of the Pb-reflector. The midplane of the moderator is foreseen for poisoning.

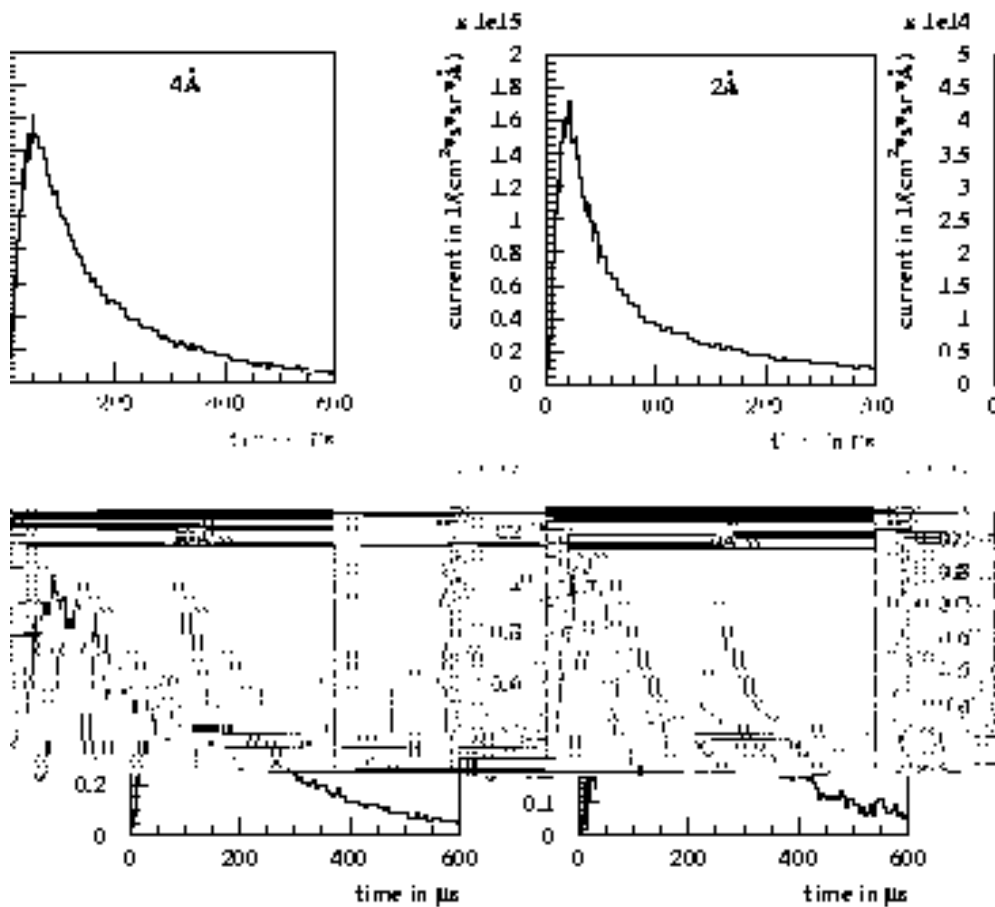


Fig. 2: Time distribution of the neutron current density for 2, 4, 6, and 10 Å for a cold coupled hydrogen moderator.

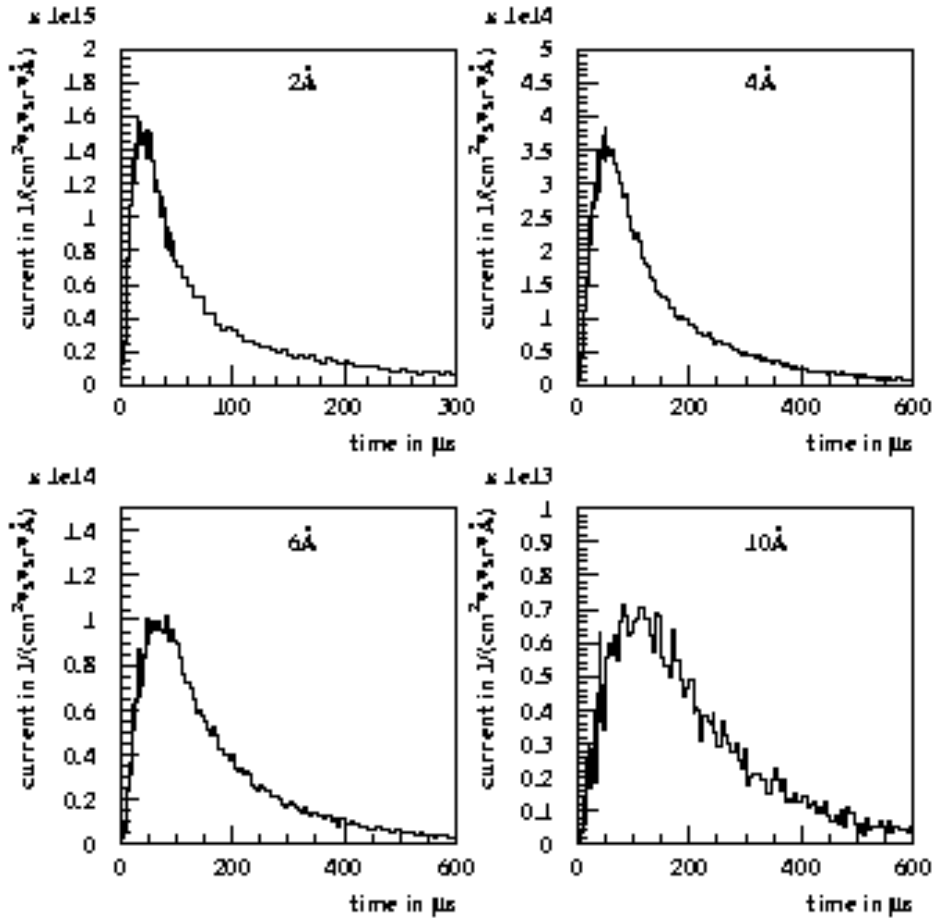


Fig. 3: Time distribution of the neutron current density for 2,4, 6, and 10 Å for a cold decoupled hydrogen moderator.

Table 2: Integrated neutron current density and peak values for 2,4, 6, and 10 Å for a could coupled hydrogen moderator.

| Wavelength   | 2 Å                   | 4 Å                   | 6 Å                   | 10 Å                  |
|--|-----------------------|-----------------------|-----------------------|-----------------------|
| Peak current neutron density<br>[ $\frac{1}{cm^2 \cdot s \cdot sr \cdot \text{Å}}$ ]       | $1.486 \cdot 10^{15}$ | $3.798 \cdot 10^{14}$ | $1.035 \cdot 10^{14}$ | $7.532 \cdot 10^{12}$ |
| Integrated neutron current density<br>[ $\frac{1}{cm^2 \cdot s \cdot sr \cdot \text{Å}}$ ] | $5.51 \cdot 10^{12}$  | $1.50 \cdot 10^{12}$  | $3.44 \cdot 10^{11}$  | $3.50 \cdot 10^{10}$  |
| Peak width FWHM [ $\mu s$ ]  | 42.79                 | 119.97                | 150.60                | 231.79                |

Table 3: Integrated neutron current density and peak values for 2,4, 6, and 10 Å for a cold coupled hydrogen moderator.

| Wavelength  | 2 Å                   | 4 Å                   | 6 Å                   | 10 Å                  |
|---|-----------------------|-----------------------|-----------------------|-----------------------|
| Peak current neutron density<br>[ $\frac{1}{\text{cm}^2 \cdot \text{s} \cdot \text{sr} \cdot \text{Å}}$ ]       | $1.515 \cdot 10^{15}$ | $3.567 \cdot 10^{14}$ | $9.549 \cdot 10^{13}$ | $7.003 \cdot 10^{12}$ |
| Integrated neutron current density<br>[ $\frac{1}{\text{cm}^2 \cdot \text{s} \cdot \text{sr} \cdot \text{Å}}$ ] | $4.70 \cdot 10^{12}$  | $1.26 \cdot 10^{12}$  | $2.89 \cdot 10^{11}$  | $2.95 \cdot 10^{10}$  |
| Peak width FWHM [ $\mu\text{s}$ ]   | 40.32                 | 92.30                 | 136.86                | 187.78                |

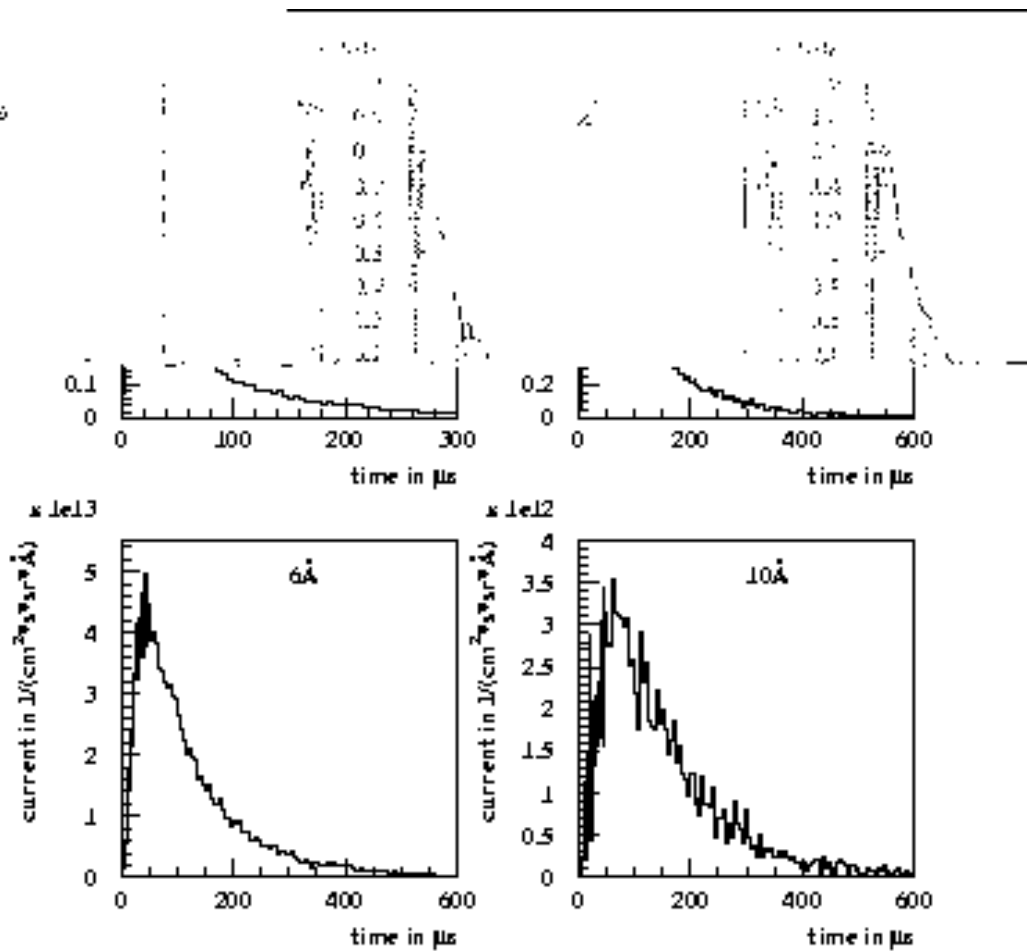


Fig. 4: Time distribution of the neutron current density for 2, 4, 6, and 10 Å for a cold decoupled-poisoned hydrogen moderator.

density and the peak values for wavelength of 2, 4, 6, and 10 Å can be found in Tab. 4. In Fig. 5 the integrated neutron current and the peak width as a function of the wavelength are plotted for each cold hydrogen moderator setup. Because of the fast lead reflector the decoupling does not result in higher time resolutions at higher wavelengths.

Table 4: Integrated neutron current density and peak values for 2,4, 6, and 10 Å for a coupled-decoupled-poisoned hydrogen moderator.

| Wavelength   | 2 Å                    | 4 Å                    | 6 Å                    | 10 Å                   |
|--|------------------------|------------------------|------------------------|------------------------|
| Peak current neutron density<br>[ $\frac{1}{cm^2 \cdot s \cdot sr \cdot \text{Å}}$ ]       | 8.546 10 <sup>14</sup> | 1.591 10 <sup>14</sup> | 4.066 10 <sup>13</sup> | 2.981 10 <sup>12</sup> |
| Integrated neutron current density<br>[ $\frac{1}{cm^2 \cdot s \cdot sr \cdot \text{Å}}$ ] | 2.44 10 <sup>12</sup>  | 5.35 10 <sup>11</sup>  | 1.20 10 <sup>11</sup>  | 1.31 10 <sup>10</sup>  |
| Peak width FWHM [μs]   | 29.71                  | 72.14                  | 93.36                  | 136.86                 |

### **AMBIENT TEMPERATURE WATER MODERATOR}**

The ambient temperature water moderator has a thickness of 5 cm. In Fig. 6 the used geometry is plotted. The time spectra of the neutron current density for a coupled moderator is shown in Fig. 7. The related numerical values for these wavelength are presented in Tab. 5.

It is decoupled with a 1 mm thick Cd-layer at the inner surface of the Pb-reflector. The spectra obtained from the simulations can be seen in Fig. 8 and the the numerical values in Tab. 6. To achieve smaller pulse widths the moderator is poisoned with a 0.5 mm thick Gd-layer in the midplane of the moderator. The time spectra of the neutron current density are plotted in Fig. 9. The values for the integrated neutron current density and the peak values for wavelength of 0.5, 1, 2, and 4 Å are given in Tab. 7. In Fig. 10 the integrated neutron current and the peak width as a function of the wavelength are plotted for each ambient temperature water moderator setup.

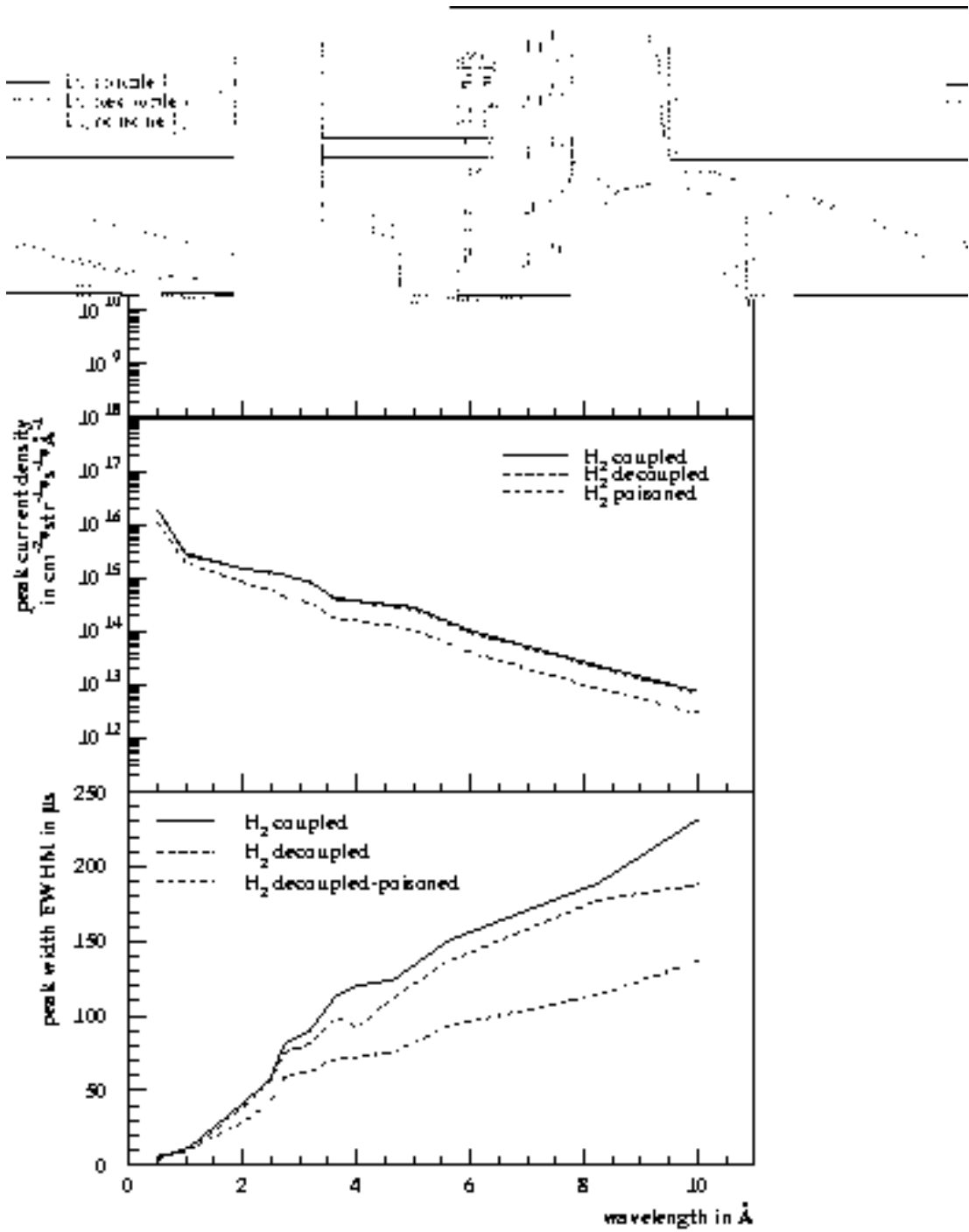


Fig. 5: The upper panel shows the integrated neutron current density, the panel in the middle the peak current and the lower panel the peak width as a function of the wavelength for a coupled, decoupled and decoupled-poisoned cold hydrogen moderator.

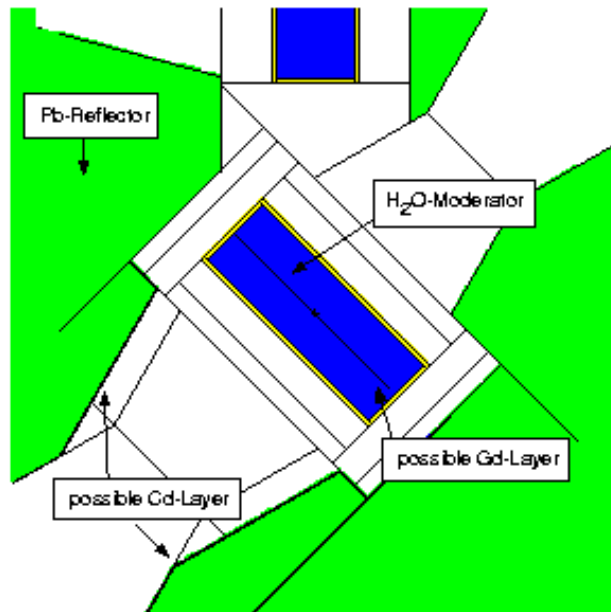


Fig. 6: Geometry of the H<sub>2</sub>O-moderator as used in the simulations. The moderator can be decoupled with a Cd-layer on the inner side of the Pb-reflector. The midplane of the moderator is foreseen for poisoning.

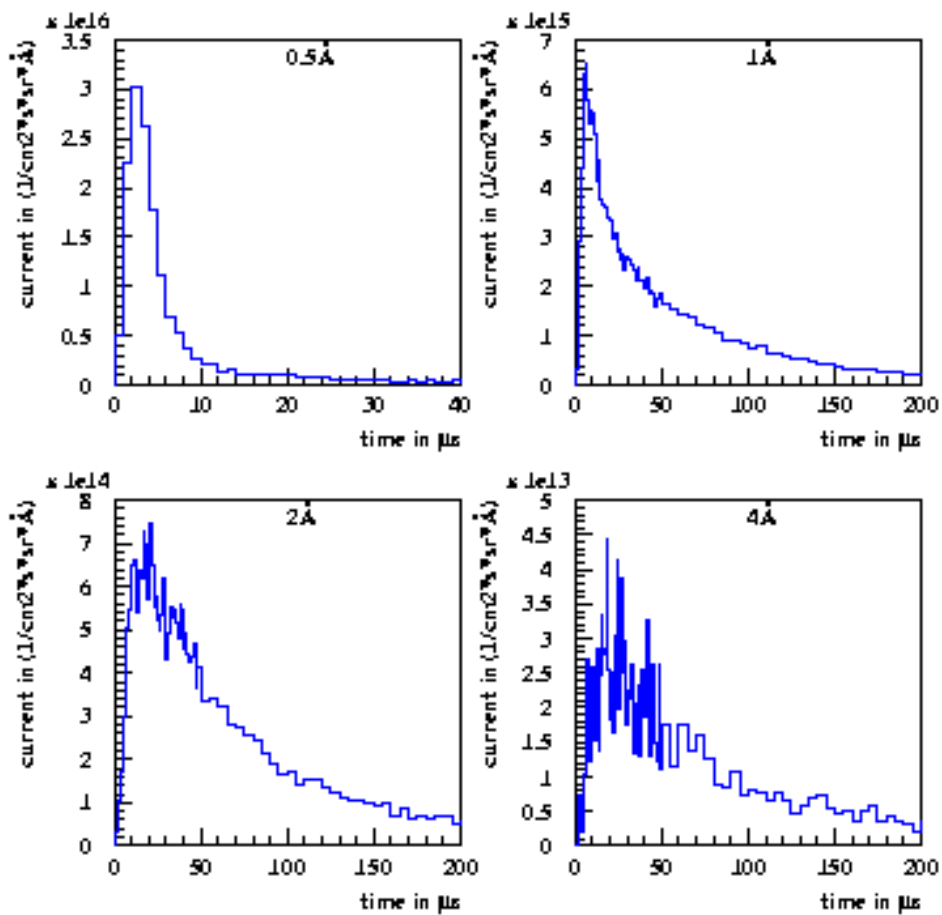


Fig. 7: Time distribution of the neutron current density for 0.5, 1, 2, and 4 Å for a coupled ambient temperature water moderator.

Table 5: Integrated neutron current density and peak values for 0.5, 1, 2, and 4 Å for an ambient temperature coupled water moderator.

| Wavelength  | 0.5 Å                | 1 Å                  | 2 Å                  | 4 Å                  |
|---|----------------------|----------------------|----------------------|----------------------|
| Peak current neutron density<br>[ $\frac{1}{\text{cm}^2 \cdot \text{s} \cdot \text{sr} \cdot \text{Å}}$ ]       | $2.86 \cdot 10^{16}$ | $6.25 \cdot 10^{15}$ | $6.26 \cdot 10^{14}$ | $2.48 \cdot 10^{13}$ |
| Integrated neutron current density<br>[ $\frac{1}{\text{cm}^2 \cdot \text{s} \cdot \text{sr} \cdot \text{Å}}$ ] | $8.05 \cdot 10^{12}$ | $1.45 \cdot 10^{13}$ | $2.79 \cdot 10^{12}$ | $1.31 \cdot 10^{11}$ |
| Peak width FWHM [ $\mu\text{s}$ ]   | 5.0                  | 19.4                 | 59.1                 | 60.9                 |

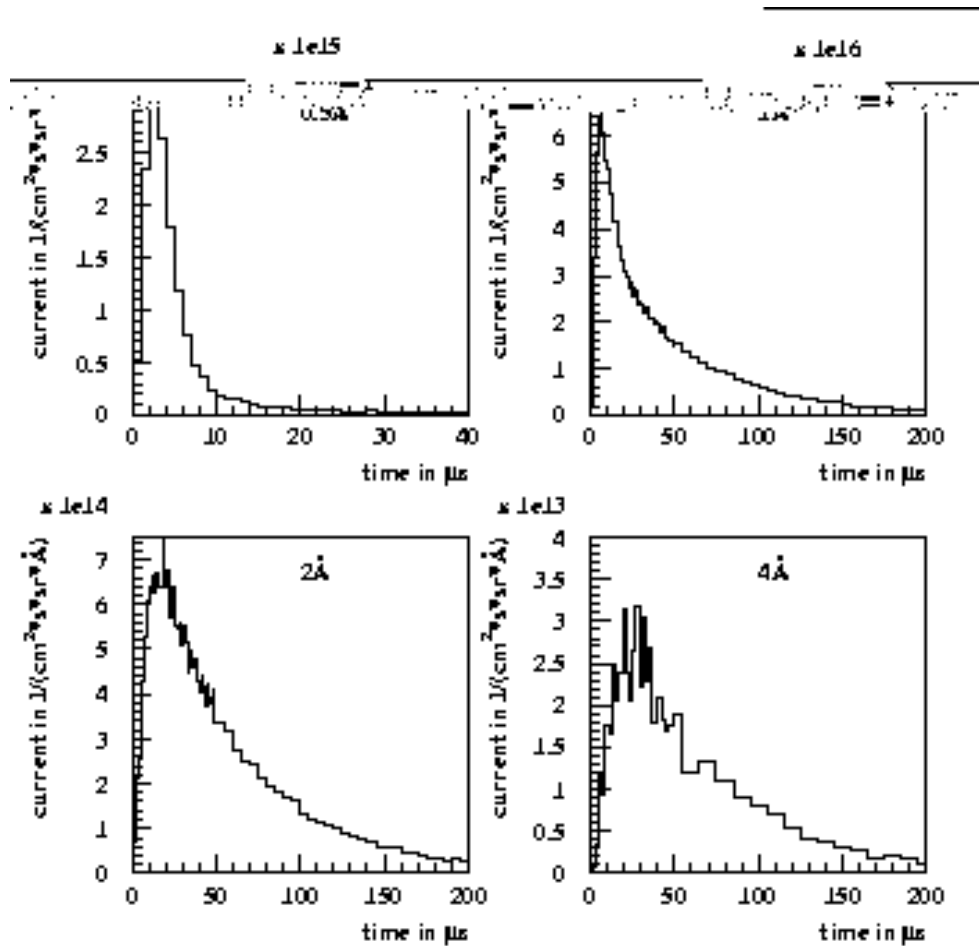


Fig. 8: Time distribution of the neutron current density for 0.5, 1, 2, and 4 Å for a decoupled ambient temperature water moderator.

Table 6: Integrated neutron current density and peak values for 0.5, 1, 2, and 4 Å for an ambient temperature decoupled water moderator.

| Wavelength  | 0.5 Å                 | 1 Å                   | 2 Å                   | 4 Å                   |
|---|-----------------------|-----------------------|-----------------------|-----------------------|
| Peak current neutron density<br>[ $\frac{1}{\text{cm}^2 \cdot \text{s} \cdot \text{sr} \cdot \text{Å}}$ ]       | $3.045 \cdot 10^{16}$ | $6.082 \cdot 10^{15}$ | $6.372 \cdot 10^{14}$ | $2.408 \cdot 10^{13}$ |
| Integrated neutron current density<br>[ $\frac{1}{\text{cm}^2 \cdot \text{s} \cdot \text{sr} \cdot \text{Å}}$ ] | $2.94 \cdot 10^{12}$  | $4.50 \cdot 10^{12}$  | $5.82 \cdot 10^{11}$  | $2.36 \cdot 10^{10}$  |
| Peak width FWHM [ $\mu\text{s}$ ]   | 3.84                  | 17.44                 | 47.17                 | 53.03                 |

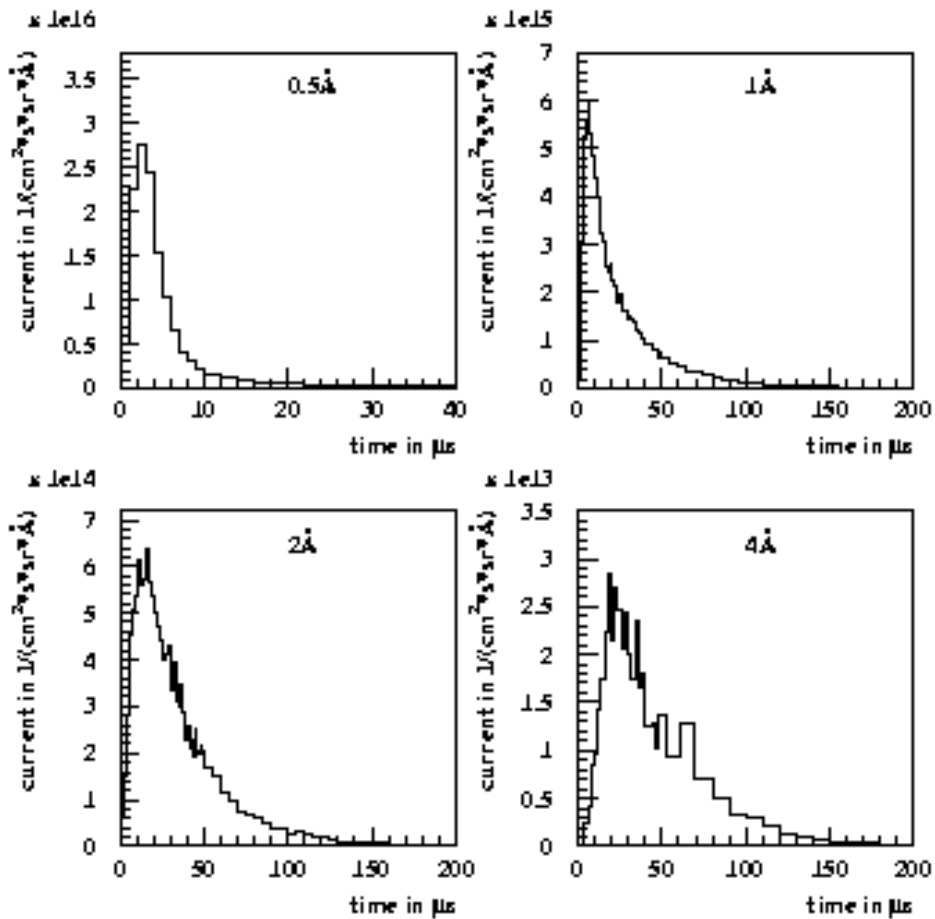


Fig. 9: Time distribution of the neutron current density for 0.5, 1, 2, and 4 Å for a decoupled ambient temperature water moderator.

Table 7: Integrated neutron current density and peak values for 0.5, 1, 2, and 4 Å for an ambient temperature decoupled-poisoned water moderator.

| Wavelength   | 0.5 Å                 | 1 Å                   | 2 Å                   | 4 Å                   |
|--|-----------------------|-----------------------|-----------------------|-----------------------|
| Peak current neutron density<br>[ $\frac{1}{cm^2 \cdot s \cdot sr \cdot \text{Å}}$ ]       | $2.436 \cdot 10^{16}$ | $5.338 \cdot 10^{15}$ | $6.190 \cdot 10^{14}$ | $2.241 \cdot 10^{13}$ |
| Integrated neutron current density<br>[ $\frac{1}{cm^2 \cdot s \cdot sr \cdot \text{Å}}$ ] | $2.81 \cdot 10^{12}$  | $2.61 \cdot 10^{12}$  | $3.33 \cdot 10^{11}$  | $1.41 \cdot 10^{10}$  |
| Peak width FWHM [μs]   | 4.25                  | 13.98                 | 30.7                  | 33.44                 |

## LONG PULSE UTILIZATION

The simulations of the neutron current leaving the viewed moderator surface are only performed for a cold coupled hydrogen moderator, because it delivers the highest intensity for cold neutrons and small peak widths are no longer of interest. The geometry is the same as for the short pulse version of the cold hydrogen moderator as shown in Fig. 1. To achieve a maximum neutron current only the coupled hydrogen moderator was considered, because decoupling and poisoning will decrease the intensity. The time dependent neutron current density is plotted in Fig. 11. Numerical values for these four wavelengths are presented in Tab. 8. In Fig. 12 the peak and integral intensity is shown as a function of the wavelength.

## POSSIBILITIES OF MODERATOR OPTIMIZATION

We see some possibilities (see list below) for further optimization of the neutronic performance of the moderators, which are shortly discussed:

- moderator thickness
- inner Be reflector
- grooved moderators
- solid methane as an advanced cold moderator
- fluxtrap target
- new scattering kernels for moderators

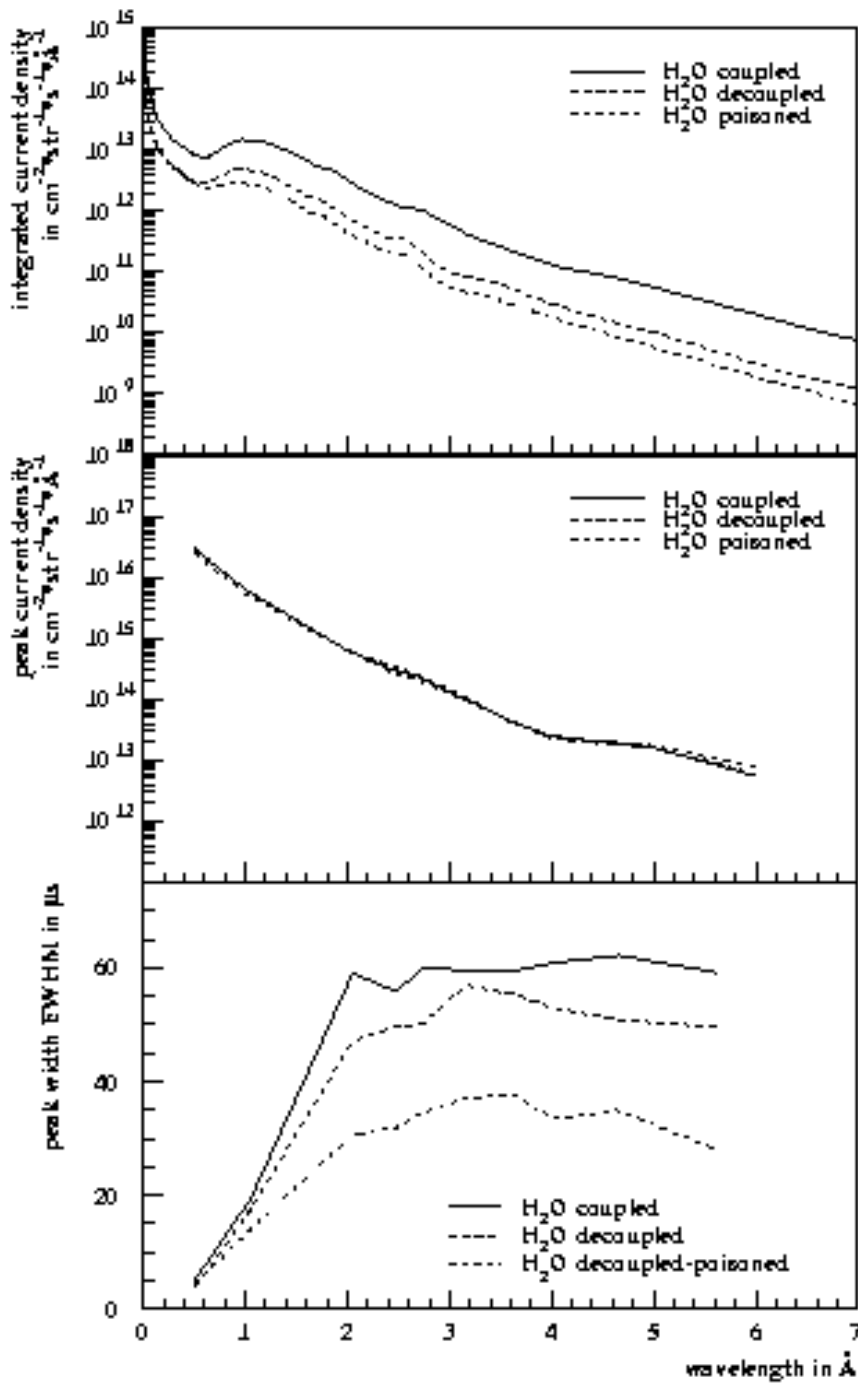


Fig. 10: The upper panel shows the integrated neutron current density, the panel in the middle the peak current and the lower panel the peak width as a function of the wavelength for a coupled, decoupled and decoupled-poisoned ambient temperature water moderator.

All optimizations are independent from the possibility of the technical realization. The discussion in this section is based on the results described in [5-8].

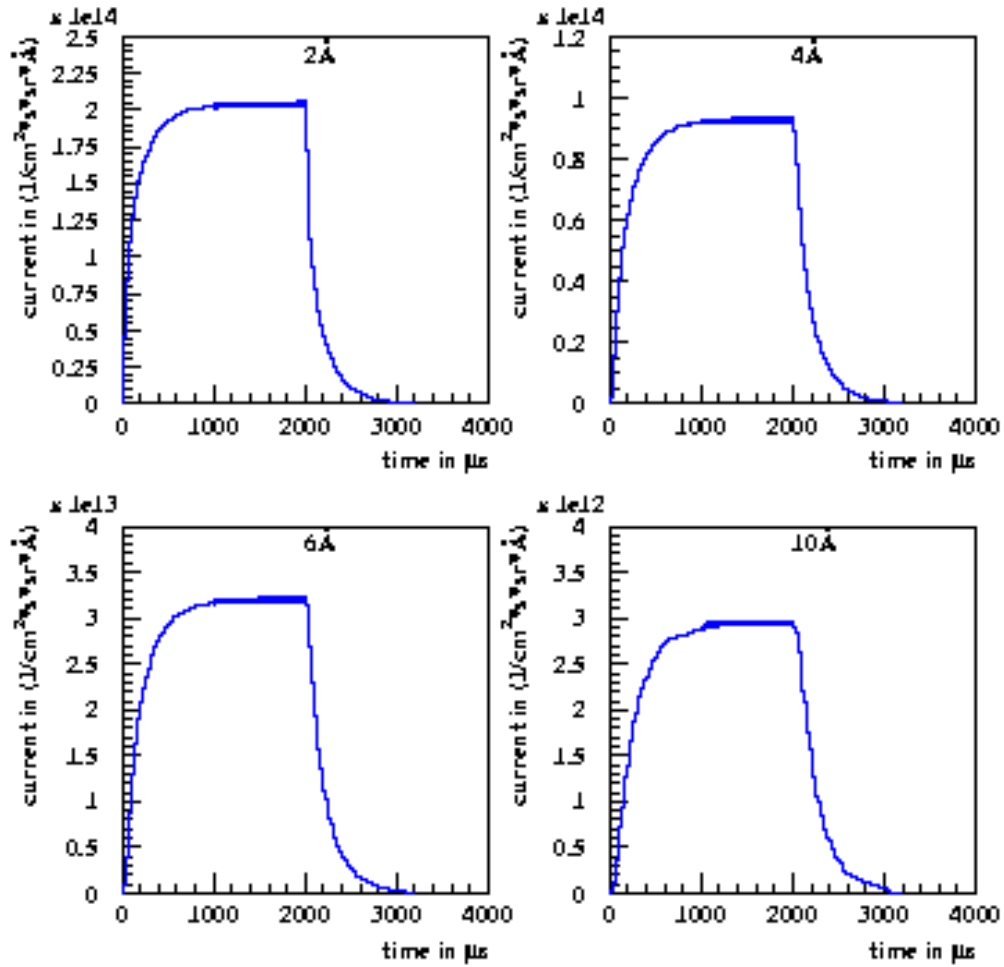


Fig. 11: Time distribution of the neutron current density 2, 4, 6, and 10 Å for a coupled cold hydrogen moderator caused by a 2 ms proton pulse.

Table 8: Integrated neutron current density and peak values for 2, 4, 6, and 10 Å for a cold coupled hydrogen moderator of a long pulse target station.

| Wavelength  | 2 Å                  | 4 Å                  | 6 Å                  | 10 Å                 |
|---|----------------------|----------------------|----------------------|----------------------|
| Peak current neutron density<br>[ $\frac{1}{\text{cm}^2 \cdot \text{s} \cdot \text{sr} \cdot \text{Å}}$ ]       | $2.05 \cdot 10^{14}$ | $9.12 \cdot 10^{13}$ | $3.12 \cdot 10^{13}$ | $2.95 \cdot 10^{12}$ |
| Integrated neutron current density<br>[ $\frac{1}{\text{cm}^2 \cdot \text{s} \cdot \text{sr} \cdot \text{Å}}$ ] | $4.17 \cdot 10^{12}$ | $1.89 \cdot 10^{12}$ | $6.53 \cdot 10^{11}$ | $6.02 \cdot 10^{10}$ |
| Peak width FWHM [μs]  | -                    | -                    | -                    | -                    |

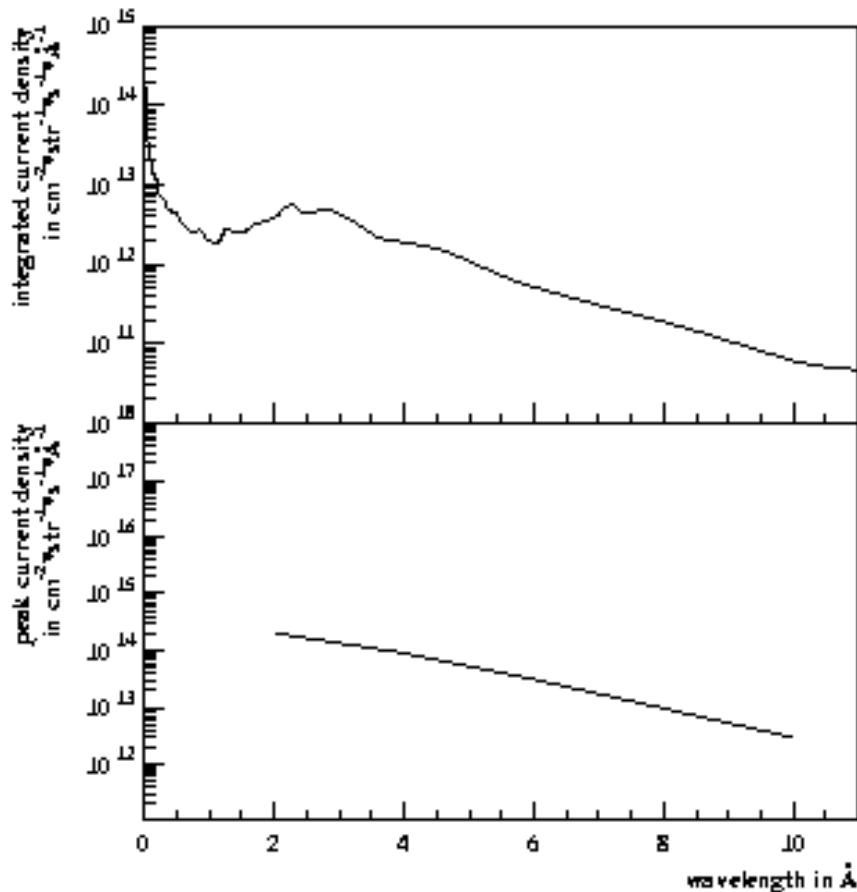


Fig. 12: The upper panel shows the integrated neutron current density, and the lower panel the peak current density as a function of the wavelength for a cold coupled hydrogen moderator for the long pulse target station.

### Moderator Dimensions and Inner Beryllium Reflector

An increase of the time integrated intensity can be achieved by increasing the thickness of the moderator [7]. The gain will be a factor of 2, when changing the thickness from 5 cm to 10 cm. But the time resolution will become worse, because the peak width (FWHM) will also increase by a factor of 2. In connection with an inner beryllium reflector with a diameter between 20-30 cm decoupling and/or poisoning could reduce the peak width (FWHM) by a factor of 2-3. This will also cause a decrease of the integral intensity by the same factor.

### Grooved Moderators

At the moment studies are performed for the neutronic performance of grooved moderators. First results show a small increase of the intensity. To compare the results with non grooved moderators the volume of the moderator material is kept constant. For a moderator with a reentry hole the

intensity is a factor of 1.5 higher than for a flat moderator. In case of a two-groove moderator a gain of a factor of 1.8 can be observed.

### **Flux Trap Target ?**

Flux trap geometry for moderators has various possibilities to increase the peak intensity in pulsed neutron spallation sources. Various experiments and simulations using flux trap moderators (extended, overlap) show that a gain factor of more than 1.5-2.0 is obtainable [9, 10].

### **Advanced Moderators**

One possibility to achieve higher intensities is the use of advanced moderator materials (methane, clathrate hydrates, ammonia, etc.). Monte-Carlo simulations show for a solid methane moderator a gain in intensity. In case of the 2 Å neutrons we observe an increase in the peak intensity of ~ 30 % compared to a cold hydrogen moderator. The peak value for a 10 Å neutron is a factor of 2 higher than the peak intensity of a cold hydrogen moderator.

## **COMPARISON WITH SNS CALCULATIONS**

We compare SNS results [5,6] with our calculations. To compare these data with our results we had to renormalize them. Therefore we changed the normalization to the energy bin width from eV to Å and renormalized to the number of protons in the ESS pulse. To take into account the higher neutron production at higher beam energies the data are normalized to the proton beam energy. When comparing the SNS data to ESS data the following differences between the both facilities have to be considered:

- different size of the moderator
- different energy of the incident proton (1 GeV for SNS and 1.334 GeV for ESS)
- SNS has an inner reflector of Be
- different position and distance between target and moderator

For comparison of the time spectra only two wavelengths were chosen, namely 2 Å and 5.7 Å in case of the cold hydrogen moderator and 1 Å and 2 Å for the ambient temperature water moderator. In Fig. 13 the ESS simulations are confronted with the SNS simulations for a coupled hydrogen moderator at 20 K. It can be seen that the peak intensity is higher in case of the ESS. The peak

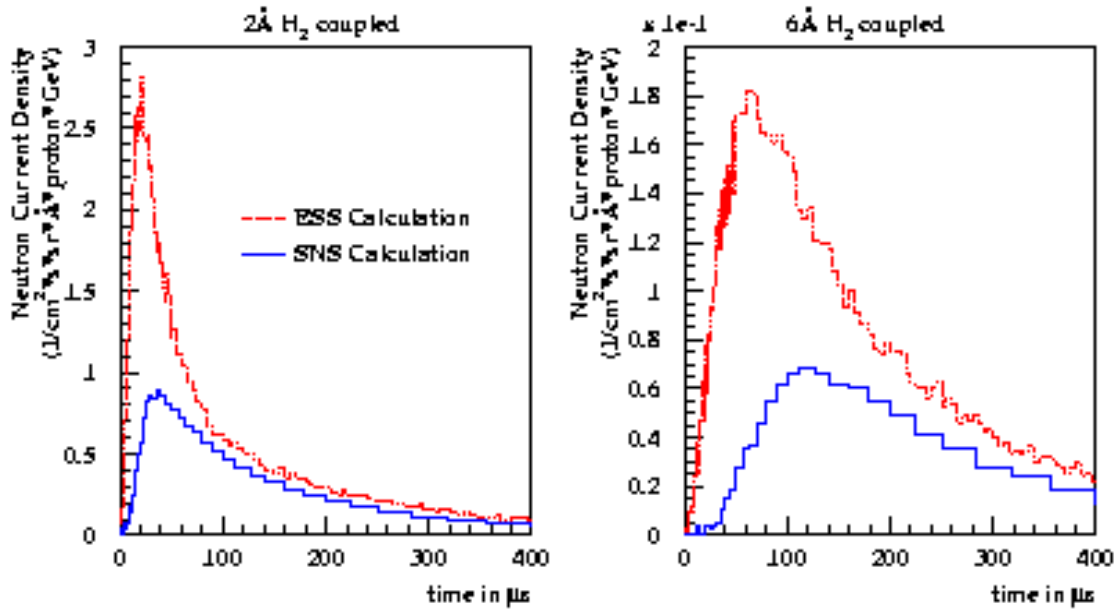


Fig. 13 Comparison between ESS and SNS of the time spectra for a coupled hydrogen moderator at 20 K.

position is shifted to later time bins. This can be due to different moderator positions. In the ESS simulation the bottom-upstream moderator position was used, whereas in the SNS simulation the moderator was placed in the top-downstream position. Looking to the spectra for the decoupled/poisoned hydrogen moderator configuration, in principal the same effect can be observed (see Fig. 14). But both spectra show the same peak position while in both simulations the moderators are located in the upstream position of the target-moderator-reflector assembly. ESS

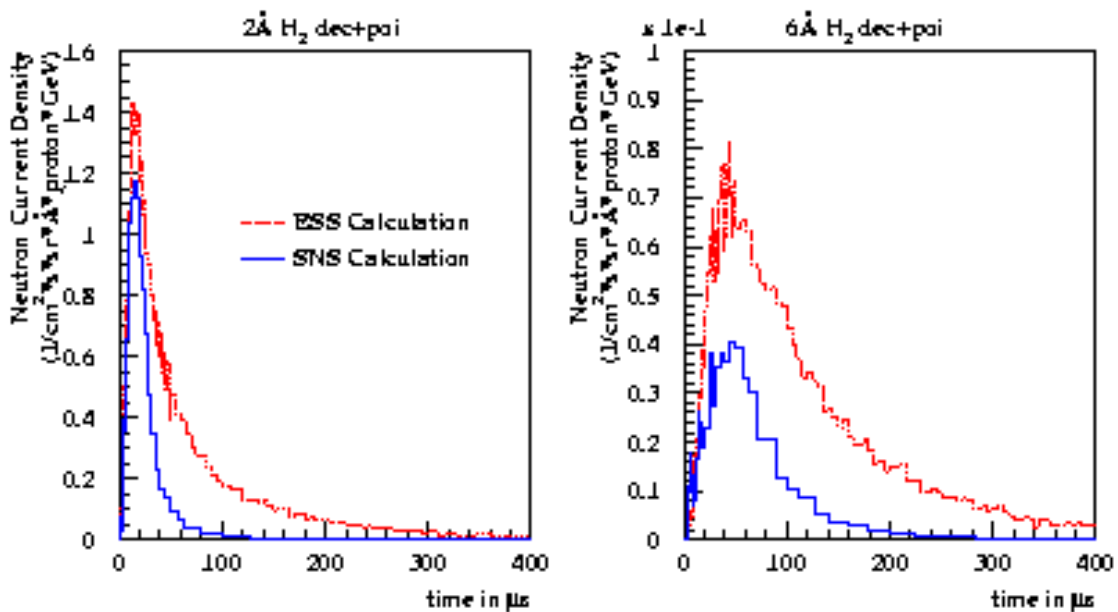


Fig. 14 Comparison between ESS and SNS of the time spectra for a decoupled-poisoned hydrogen moderator at 20 K.

delivers higher peak values for a cold hydrogen moderator and also for the ambient water moderator. As can be seen in Fig. 15 the ESS data show higher values for the peak intensity and the same peak position as the SNS data. Here also two different moderator positions are used. In the SNS the decoupled-poisoned water moderator is placed at the bottom-downstream position.

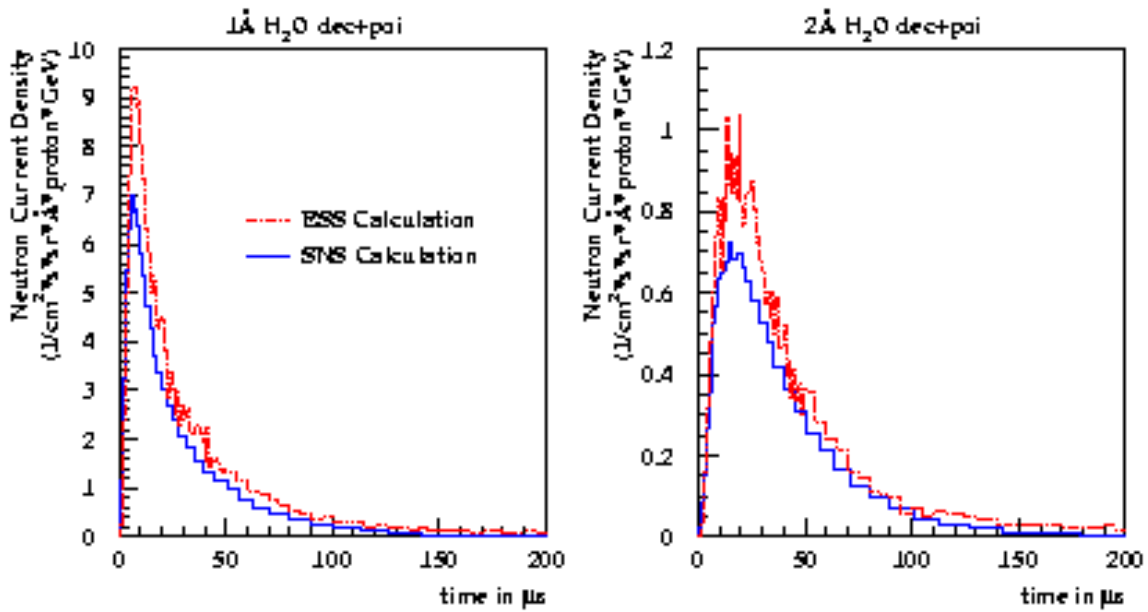


Fig. 15 Comparison between ESS and SNS of the time spectra for a decoupled-poisoned water moderator at ambient temperature.

## References

1. D. Filges et al., A First Attempt to Estimate the performance of the ESS Moderators for the Short Pulse Target Station. ESS-SAC-MOD-No.:1, 23 November 2000.
2. D. Filges et al., H<sub>2</sub> and H<sub>2</sub>O Moderator Neutron Performance Monte-Carlo Simulations for the ESS Reference Target-Moderator-Reflector-System. ESS-SAC-MOD-No.:2, 22 February 2001.
3. ESS Volume III, The ESS Technical Study. ISBN 090-237-6-659, November 1996.
4. S.M. Bennington, ESS Moderator Summary. private communication, Meeting at Heathrow, U.K., 16 February 2001.
5. E.B. Iverson, Comparison of Composite and Water Moderator Performance at SNS. SNS/TSR-202, 25 September 2000.
6. E.B. Iverson, Detailed SNS Neutronic Calculations for Scattering Instrument Design. POI5 Configuration. SNS/TSR-203, 13 September 2000.
7. T.Kai et al., Optimization Study of Coupled Hydrogen Moderator with Extended Premoderator, 15th Meeting of the International Collaboration on Advanced Neutron Sources, November 2000.
8. E.B. Iverson et al., Hydrogen-Water composite moderators at pulsed spallation neutron sources. Proceedings of the AccApp00 conference, November 2000.
9. G.J. Russell et al., ICANS IX, p.177, Villigen, Switzerland, September 1986.
10. Y. Kiyonagi et al., NIM A 343(1994), 550-557.